Towards microfluidic-based depletion of stiff and fragile human red cells that accumulate during blood storage

Sha Huang[1], **Han Wei Hou**[1,$], **Tamir Kanias**[3], **JT Sertorio**[3], **Huichao Chen**[5], **Derek Sinchar**[3], **Mark Gladwin**[3,4], and **Jongyoon Han**[1,2,*]

[1]Department of Electrical Engineering and Computer Science, Massachusetts Institute of Technology, Cambridge, MA, USA

[2]Department of Biological Engineering, Massachusetts Institute of Technology, Cambridge, MA, USA

[3]Vascular Medicine Institute, University of Pittsburgh, Pittsburgh, PA, USA

[4]Department of Medicine, Division of Pulmonary, Allergy and Critical Care Medicine, University of Pittsburgh School of Medicine, Pittsburgh, PA, USA

[5]Harvard School of Public Health, Boston, MA, USA

Abstract

In this study, the effects of prolonged storage on several biophysical properties of red blood cells (RBCs) were investigated. Single cell deformability was used as an important criterion in determining subgroups of RBCs evolved during storage lesion. A deformability-based microfluidic cell sorting technology was applied, which demonstrates the ability to enrich and separate the less deformable subpopulations of stored blood. These less deformable RBC subpopulations were then associated with other important markers such as osmotic fragility indicating cell integrity as well as microparticle content. This work demonstrates a systematic methodology to both monitor and improve banked blood quality, thereby reducing risks related to blood transfusion.

INTRODUCTION

Blood transfusion is one of the most common and lifesaving medical therapies.[1] Every year in the United States alone, close to 5 million people need blood transfusion and approximately 14 million units of blood are collected and transfused.[2] According to the Food and Drug Administration (FDA) regulation, refrigerated red blood cells (RBCs) can be stored up to 42 days. However, strong inter-donor differences exist, as some stored RBCs were observed to degrade early, well before the six-week limit.[3, 4] Significant loss of RBC deformability typically occurs after 3 weeks of storage time due to adenosine triphosphate (ATP) and 2,3-diphosphoglycerate (DPG) depletion.[5, 6] Poorly deformable RBCs could give rise to microcapillary obstruction[7] and massive post-transfusional RBC clearance.[8–10]

*Corresponding Author: Jongyoon Han (jyhan@mit.edu).
$Current Address: Lee Kong Chian School of Medicine, Nanyang Technological University, Singapore.

Increased RBC clearance in spleen as well as hemolysis, often observed posttransfusion[9, 11–14], are believed to pose added risk of blood transfusion.[11]

However, studies suggest not all stored RBCs are unfit for transfusion that a majority of stored RBC stay in circulation following the initial accelerated clearance during the first 24 hours has been observed in humans before being observed in mice.[8] It is possible that the rapid RBC removal is associated with splenic mechanical retention of more rigid RBC subgroup from the old stored blood, as suggested by Deplaine et.al.[9] A separate work by Huang et.al also demonstrated on a malarial mice model that increased RBC stiffness associated with increased spleen mass and RBC retention.[15] Impaired deformability, therefore, may be an important biomarker for the old stored RBC subpopulation to be cleared post transfusion.[9, 15]

Besides mechanical retention in spleen, hemolysis and the formation of microparticle-encapsulated hemoglobin (i.e. MPs)[16] are considered as another important pathophysiological outcome of storage legion of transfused RBCs. Hemolysis products, including cell-free hemoglobin and RBC MPs, impair vascular function and activate the hemostatic system, via accelerated nitric oxide scavenging and generation of reactive oxygen species.[16, 17] The accumulation of exocytic microvesicles or MPs leads to increased infection risks, or in severe scenarios, multiple organ failure and death.[14, 16, 18] Experiments with canine RBC concentrates noted a 1.8-fold increase in MP concentration over 35 storage days[16, 19], confirming the strong link of storage time and MP production. However, it remains unclear whether hemolysis and MP formation occur more preferably to a certain subgroup of these old stored RBCs: for example, hemolysis is known to be attributed by the loss of RBC membrane integrity[16], and the latter also induces increased RBC stiffness as observed in ATP depletion studies[20]. An important question to ask would be whether RBCs with impaired deformability are more susceptible to hemolysis. More specifically, we are interested in two issues here: first, whether dissimilar deformability subgroups would emerge from the same population over storage time and second, whether these deformability subgroups would exhibit differential susceptibility to *in vivo* post-transfusion hemolysis.

Given the critical importance of RBC deformability in blood storage as well as microcirculation in general, several techniques have been developed in the past to measure the changes in RBC deformability during blood storage lesion, including ektacytometry[21], a laser diffraction based measurement through subjecting RBCs to "varying shear stress in suspending media"[22] or micropore filtration[23]. However, these measurements reflect only bulk properties of RBCs, and are unable to reveal single cell or subpopulation-level information. To efficiently predict bulk-level RBC survival rate post transfusion, the first objective is to determine RBC characteristics at single cell level, and subsequently we project whether a given RBC can survive in microcirculation. It is noted that existing single cell measurements such as micropipette aspiration[24], diffraction phase microscopy[25], and optical tweezers[26] are limited by their low throughput. Moreover, they are unsuitable to describe population-wide deformability shifts for stored RBCs, where multiple subpopulations with dissimilar morphologies may coexist.

More recently, there has been remarkable interest and significant development on measuring RBC deformability using a microfluidic platform. For example, Bow *et.al* developed a RBC "deformability cytometer" measuring the transit velocity of RBCs traversing narrow bottleneck structures. Significant impairment in RBC deformability was observed after malaria parasite infection[27]. In a separate study, Kwan et. al reported a "Funnel Chain" system, which quantifies cell deformability by the threshold pressure required to deform individual RBCs through narrow constrictions.[28, 29] This system is similar to a single cell level filtration system, and the critical device dimension of 2 μm closely recreates typical gap size of human splenic slits.[28] Overall, the notable system high-throughput and the ability to provide population-wide single cell information make microfluidic platforms favorable for deformability-based blood diagnostic.

In this paper, we employed the deformability cytometer to characterize stored RBC deformability and determined the evolution and redistribution of RBC deformability subgroups in order to gain a better understanding of blood storage lesion. Moreover, we developed a novel biomimetic blood separation system which could efficiently enrich and remove the less deformable RBC subgroups (along with MPs) and associated them with other clinically important hemolysis markers such as RBC fragility. By further optimizing our current sorting technology, we believe that blood shelf life can be extended and transfusion related clinical risks can be minimized.

METHOD AND MATERIALS

Microfluidic device design and fabrication

Two novel microfluidic devices were introduced in this project, namely the deformability cytometer[30] and the deformability sorter.[31] The detailed designs of both devices were illustrated in Figure S1A and Figure 2 respectively. Briefly, the deformability cytometer consisted of repeated constrictions with gap size of 3 μm and channel height of 5.3 μm. The gap size enabled RBCs to undergo substantial deformation, mimicking in vivo microcirculation[15] and the channel height was careful chosen such that all RBCs including the spherocytes would not be constrained by the device height, entering the main channel, whereas other blood cell types with diameter above 6 μm would be stopped in the reservoir, minimizing potential clogging downstream.

The deformability sorter attempted to mimic the *in vivo* margination effect in blood capillaries[32]. The critical channel length (i.e. between A to B in Figure 3) was 2cm, to allow sufficient lateral displacement. The expansion zone between B and C in Figure 3 was introduced to clearer separation into two distinct compartments. Channel width and height were chosen to be 20 μm X 10 μm, which were comparable to *in vivo* capillary size.

All microfluidic devices were fabricated in polydimethylsiloxane (PDMS) using standard microfabrication and soft-lithographic techniques described previously.[30, 32] Briefly, patterned silicon wafers were silanized with trichloro (1H,1H,2H,2H-perfluorooctyl) silane (Sigma Aldrich, St Louis, MO) and PDMS prepolymer (Sylgard 184, Dow Corning, Midland, MI) mixed ratio with curing agent in 10:1 (w/w) were poured onto the wafer to cure for 1–2 h at 80 °C. For the deformability sorter, a second cast was required to give the

final PDMS microchannels. Holes (1.5 mm) for fluidic inlets and outlets were punched and the PDMS devices were irreversibly bonded to glass slides using an air plasma machine (Harrick Plasma Cleaner, Ithaca, NY).

Microfluidic device operation and data acquisition

Blood bank units from healthy donors containing packed RBCs (60~70% hematocrit) (Research Blood Components, Brighton, MA) were stored in sterile conditions at 4 °C to different aging period. Leucodepletion was performed at blood bank within an hour of fresh blood collection. Prior experiments, blood samples were carefully withdrawn from the package with a 23 gauge needle and adjusted to physiological hematocrit (~45%) in sample buffer containing $1\times$ PBS.

The deformability sorting device was mounted on an inverted phase contrast microscope (Olympus IX71) equipped with a Hamamatsu Model C4742-80-12AG CCD camera (Hamamatsu Photonics, Japan) for imaging of blood flow. Blood samples were pumped through the device using a syringe pump (PHD 2000, Harvard Apparatus, Holliston, MA) at $5\ \mu\text{Lmin}^{-1}$. After the flow had stabilized, samples were collected from the center and side outlets for subsequent analyses.

RBC samples were then further spun at 300g for 1 min and resuspended in 1X PBS buffer solution containing 1% BSA so that confounding effect due to the non-specific interaction between RBC and the device components can be minimized. The final hematocrit was between $0.1 – 1\%$ for deformability analysis. When the deformability cytometer was mounted on the same microscope set up, diluted RBC samples were loaded to the inlet reservoir and the flow was driven by pressure gradient as described[30]. RBC flow was recorded by the camera and individual cell velocity (or deformability) was post-analyzed with image J.

Osmotic fragility

Evaluation of RBC osmotic fragility in unsorted and sorted (center/side) RBC specimens was determined using a modified Pink Test assay.[33, 34] Unsorted or sorted RBC specimens were washed one time ($1500\times$g, 10 min, 18 °C) to remove supernatants, and packed RBCs were suspended with Pink Test solution (a hypotonic Bis-Tris buffer containing 25 mmol/L sodium chloride, 70 mmol/L Bis –Tris buffer, and 135 mmol/L glycerol; pH 6.6) to a final HCT of approximately 1.6 %. The RBCs were incubated at room temperature for 24 h. After the incubation period, each RBC sample was centrifuged ($1500\times$g, 10 min, 18 °C) and the concentration of free hemoglobin (μmol/L) in samples supernatants was determined by the Drabkin's reagent method.[35] Percent osmotic hemolysis was calculated as follows:

$$\text{Osmotic hemolysis }(\%) = \frac{Hb_{supernatant}}{Hb_{total}} \times 100$$

whereas $Hb_{supernatant}$ is the concentration of free Hb (μmol/L) from RBC supernatants following Pink Test, and Hb_{total} is the total amount of Hb (μmol/L) of each RBC sample.

Reagents used for Red Blood Cell Microparticles quantification

Megamix™, a mixture of monodisperse fluorescent beads of three diameters (0.5, 0.9 and 3 μm), was purchased from BioCytex (Marseille, France). Flow Cytometry Absolute Counting Standard microbeads (7.6 μm) were purchased from Bangs Laboratories, Inc. (Fishers, IN). Annexin V FITC, Glycophorin A-PE, Mouse IgG$_{2b}$k-PE isotype control, and annexin V-binding buffer concentrate were purchased from BD Pharmingen (San Jose, CA).

Quantification of Red Blood Cell Microparticles

A detailed method for isolation and quantification of red cell microparticles (RBC MPs) has been previously described[36, 37]. Briefly, each sample consisted of 25 μL plasma, 1μL mouse anti-human CD235a-PE, 5 μL Annexin V FITC and 69 μL of Annexin V-binding buffer for a total volume of 100 μL. Each sample was incubated for 30 minutes at 4°C, protected from light and 400 μL of Annexin V-binding buffer was subsequently added to the sample preparations. Immediately prior to flow cytometric analysis, 150 μL of a master bead mixture consisting of one volume of absolute counting beads (7.6 μm) to two volumes of Megamix™ was vortexed and added to each tube for a final volume of 650 μL. Acquisition for each sample was set to achieve 1000 events of the 3 μm beads. Red cell MP enumeration was obtained on a LSRFortessa flow cytometer (BD Biosciences, San Jose, CA).

RBC MPs were defined as CD235a-PE+ Annexin V+ events conforming to a light scatter distribution within the 0.5 μm to 0.9 μm bead range. A discrete population of CD235a-PE+ Annexin V+ events was first identified in the PE × FITC dot plot. By back gating, the position of the CD235a+ Annexin V+ population could be confirmed relative to the distribution of calibration beads in both the PE x FSC window and the SSC x FSC window. Isotype control labelling of samples with mouse IgG$_{2b}$k-PE confirmed specificity of Glycophorin A-PE (CD235a- PE+) labelling of MPs. Calculation of MP counts was based upon the following equation:

$$\text{MP counts} = \text{Absolute number of } 7.6\mu m \text{ beads} \times \left(\frac{number\ of\ MP\ events}{number\ of\ 7.6\mu m\ beat\ events} \right)$$

RESULTS

Changes in RBC deformability over storage time

Banked RBCs from three healthy donors were analyzed using a microfluidic deformability cytometer consisting of repeated bottleneck structures as described by Bow *et al* (Figure S1A).[30] High transit velocity corresponds to good deformability and *vice versa*, which can be obtained as a quantitative metric of individual RBC's ability to squeeze through tiny splenic slits and remain in circulation. [10, 15] Significant RBC stiffening was observed for all three donors (Donor 1–3, black, blue and red circles) between 21 and 28 days of storage (Figure 1A). The overall trend of stored RBC stiffening was consistent with other bulk measurement tools such as ektacytometry.[3]

Figure S1B reveals the population-wide single cell information obtained from the same experiments, where each dot represents the passing of one RBC. It was found that not only

the average RBC velocity decreased drastically between week 3 and 4, but also the velocity distribution shifted from a unimodal normal to a heavy-tailed distribution (Figure 1A, inset). It is evident that even after 5 weeks of storage, there still exists a significant subgroup of RBCs with a similar deformability as compared to fresh stored RBCs.

Suppose that the post-transfusion survival for fresh (1-week-old) stored RBCs is 95% according to previous studies on mice[11], we then drew a velocity threshold at 2.5, marking the threshold for stiffest 5% of freshly stored RBCs. It is presumed that RBCs with velocity below the threshold value are likely to be cleared post transfusion through splenic mechanical retention.[9, 15] The percentage of RBC clearance was then estimated in Figure 1B that a sharp increase in retention percentage was seen after 21 days of storage. Furthermore, old RBCs stored over 28 days were projected to have a survival rate around 50%, consistent with an independent mice study in which 60% of old stored RBC were reported to survive post transfusion.[11]

The significant deformability drop is accompanied by time-dependent RBC morphological changes. After 4 weeks of storage, a significant percentage of stored RBCs transformed into echino-spherocytes (Figure 1C and S1C) and were considerably stiffer as compared to the discocytes commonly seen in fresh blood.[20]

Changes in RBC fragility over storage time

Parallel with single RBC deformability characterization, bulk level RBC osmotic fragility measurements were performed over storage time. Osmotic fragility measures the percentage of hemolysis that occurs when RBCs are subjected to osmotic stress. The measurement reflects the extent of membrane integrity and is heavily affected by RBC surface area to volume ratio (S/V).[38] During storage lesion, increased fragility can lead to a higher likelihood of *in vivo* RBC breakdown, contributing to added risk of blood transfusion.

Figure 1D illustrates the time-dependent increase in osmotic fragility among four healthy donors up to 40 days. Though significant inter-individual differences existed in the fresh stored RBCs, the rate of increase in osmotic hemolysis was fairly similar across all donors (slope = 0.62± 0.13, linear regression).

The increase in osmotic fragility over storage period could be related to RBC surface transformation. It has been documented that an abnormally high osmotic fragility often associate with clinical conditions such as spherocytosis or hypernatremia[39]; in both situations the blood contains a significant fraction of crenated RBCs (i.e. echino-spherocytes). Besides, a sharp increase in osmotic fragility was also observed during discocyte-echinocyte transformation.[40] In our study, significantly increased proportion of echino-spherocytes was observed during the late storage period (Figure 1C). These echino-spherocytes are believed to be associated with a reduced S/V[41] and membrane integrity[42] and may be responsible for the overall increase in bulk-level osmotic hemolysis.

Deformability-based RBC sorting device

To further correlate dissimilar deformability subgroups with corresponding blood hemolysis characterizations, a microfluidic deformability-based RBC sorter was developed to enrich

and separate the less deformable RBCs from old stored blood using the concept of blood margination.

The device consists of an inlet, a filtration region, a margination region of 2 cm × 20 μm × 10 μm (length × width × height) microchannel, an expansion region, and the center and side outlets (Figure 2). The margination effect took place in the 2 cm long microchannel, where the more fluidic-like deformable RBCs occupied the channel center, displacing stiff RBCs away from the axis center. As the stiff RBCs marginalized to the side walls, they then could be collected from the side outlet, achieving high throughput RBC sorting. The width of outlet channels were designed to be 1:8:1. A similar version of this device employing the same principle has been reported earlier by Hou *et al*.[32]

To illustrate that the device is capable of enriching and separating different deformability subpopulations of healthy RBCs, we pre-stained some old RBCs (31 storage days) with calcium Fluo4 dye and then mixed them well with more deformable fresh RBCs (4-day-old) at 1:9 ratio. When passing the blood mixture through the margination device, old RBCs appeared as fluorescent dots whereas fresh RBCs were seen as dark backgrounds (Figure 2). Fluorescence-based flow cytometry (FACS) subsequently confirmed that the sample indeed consist of two distinct subpopulations in which 89.8% of the RBCs showing extremely low fluorescence signal (i.e. the fresh RBCs, unstained) whereas 10.2% of the RBCs exhibiting high fluorescence intensity (i.e. the old RBCs, Fluo4 stained). Initially, the blood mixture was first loaded into the device inlet, and the fluorescent RBCs (i.e. old RBCs) were evenly distributed across the channel width (Region A, blue). As RBCs moved along the straight channel (margination zone), the fluorescence RBCs slowly migrated towards the channel sidewalls (Region B, green). Finally, the fluorescent RBCs were concentrated to the side channels (Region C, orange). FACS analysis using Accuri™ C6 flow cytometer (BD Biosciences, San Jose, CA) confirmed that the sample collected from the side channel consisted of 26% fluorescent RBCs (i.e. old RBCs), a 3-fold enrichment as compared to 10.2% in the original blood mixture.

Redistribution of RBC deformability subgroups after sorting

Four to six week-old banked RBCs from different healthy donors were passed through the microfluidic deformability sorter as described above. RBC velocities at center and side outlets were normalized against the inlet velocity specific to each donor sample. The pooled effect on RBCs deformability after sorting was shown in Figure 3A: cells collected from the center outlet exhibited a normalized velocity of 1.13, slightly higher than the unsorted control ($p<0.05$), whereas the normalized velocity for cells collected from the side outlet was only 0.73, 23% less deformable than the unsort control ($p<0.001$). The effect of deformability based blood sorting on 6 individual donors is presented separately in Figure S2A. We note that although our device was designed to have multiple lanes to minimize any clogging issues, some old stored blood samples contained significant amount of very stiff cells and clogging did become a concern which limited our sample throughput. We had to stop collecting data before device blockage, which accounted for the much fewer cells being captured towards prolonged storage period.

The deformability-based sorting also led to a significant shift in overall RBC deformability distribution (Figure 3A), that an increased fraction of stiff RBCs were apparent in the side outlet. Using the same approach described in Figure 1A, we hypothesized a normalized threshold velocity at 0.8, such that around 40% of the unsort RBCs fell below this threshold [11]. Whereas both unsort and center channels exhibited a similar percentage of RBCs moving below this threshold velocity (41.2% and 38.9% respectively), an increase over 1.6 fold in the percentage of stiff RBCs were found in the side channel (65.5% of RBCs fell below given threshold velocity). The result again confirmed that through margination and Fahraeus effects (i.e. more efficient migration in small channel size)[31], less deformable RBCs were concentrated in the side outlet.

One important RBC clearance mechanism *in vivo* is the mechanical trapping of cells in spleen. In this work, we employed a microfluidic RBC deformability cytometer to estimate the rate of RBC retention in spleen.[15] Less deformable RBC subgroups are more likely to be removed through splenic trapping. [9, 15, 43]

To quantitatively evaluate the effect of blood sorting on deformability distributions, we used three independent approaches to identify the less deformable RBC subgroups that are more likely to be trapped *in vivo* in spleen: 1) rely on other clinical studies to determine a threshold velocity[15] below which RBCs are considered as less deformable; 2) perform clustering analysis to obtain the deformable and stiff RBC subgroups; and 3) use a statistical model to resolve the single RBC velocity into bimodal distributions. In the first approach, the threshold velocity in Figure 1 & 3 was estimated based on previous studies by Hod *et al.*[11], in which the authors reported approximately 5% of RBC clearance after fresh RBC transfusion. We therefore marked the slowest 5% of RBCs based on our fresh RBC velocity profile and applied the same value for subsequent stored RBCs. This crude threshold velocity estimation worked surprisingly well that the projected percentage of old stored RBC survival matched reported values from independent sources.[9, 11]

The second approach to decide RBC subgroup distributions was to cluster our single cell deformability using the K-means algorithm[44]. In Figure 3B, the red dots represent RBC clusters that are sufficiently deformable and therefore unlikely to be removed, whereas the black dots represented RBC clusters with low deformability and are more likely to be removed. The percentage of RBCs below critical velocity, or the percentage black dot clusters in unsort, center and side channels were 41.8%, 40.7% and 71.8% respectively, matching our estimated values from the first approach.

The third approach to estimate threshold velocity is based on statistical model. We fit the velocity profile with mixture model distributions and estimate the retention rate based on the relative ratio of each distribution. More specifically, the following probability density function was used in our analysis:

$$f(x) = a_1 \frac{1}{\sqrt{2\pi}c_1} e^{-\frac{(x-b_1)^2}{2c_1^2}} + a_2 \frac{1}{\sqrt{2\pi}c_2} e^{-\frac{(x-b_2)^2}{2c_2^2}} \quad (1)$$

where $0 < a_1 < 1; a_1 + a_2 = 1; b_2 > b_1; c_1 > 0;$ and $c_2 > 0$.

After log transformation, the normalized velocity data in Figure 3A was re-plotted in Figure 3C, in which the velocity of RBC collected from unsort, center and side channels can each be represented by a bimodal distribution. The fraction of stiff RBCs (i.e. subpopulations that are likely to be cleared) was denoted by a_1 and all the parameters were estimated by the maximum likelihood (ML) method.[15]

Based on this estimation, the fraction of stiff RBCs in the unsorted inlet was 33%, similar to the RBC retention rates reported in the literature (30%–40%).[9, 11] The fitting also suggested a significantly larger fraction of 58% of stiff RBCs in the side outlet, consistent with our projected numbers using other approaches (table 1).

We would also note that in the last approach, though the fraction of stiff RBCs (i.e. a_1) is similar for unsorted and center RBCs (0.33 vs. 0.38), the mean value of the high-velocity subpopulation b_2 improved significantly from 0.27 to 0.51 after passing through the sorting device (table 1). The result suggests the promising potential of further purify and enrich the more deformable RBC in the center outlet for clinical benefits.

Sorting effects on RBC morphology, osmotic fragility, and microparticle concentrations

The effects of sorting on RBC morphology, osmotic fragility and microparticle concentrations were also investigated. Given the large inter-individual variation, the percentage of discocytes in the center and side outlets were normalized against the inlet control for each blood sample and the final discocyte count were presented as the relative increase or decrease compared to corresponding control (Figure 4A). A significant decrease in the percentage of discocytes was observed in all samples collected from the side channel ($p<0.05$, paired t-test). However, no significant difference in the discocyte count can be concluded between the unsort and center outlets. The un-normalized fraction of discocytes in individual blood samples are shown in Figure S3.

Figure 4B shows the osmotic fragility percentage measured from the unsorted inlet as well as the center and side outlets. RBCs collected from the side channel exhibited much higher osmotic fragility than the control and center channels ($p<0.05$, paired t-test, Figure 4B both panels). It is also noted that the sorting was also found to be more effective on late storage RBCs (>28 day storage, Figure 4B left panel). A slight but significant improvement on RBC fragility collected from center outlet was still observed for RBC stored over 28 days ($p<0.05$, paired t-test). The effect of sorting on individual blood fragility is presented in Figure S4 A.

The margination cell sorting device will also enrich plasma-borne factors and small particles into the side outlet channels. The effect of sorting on microparticle count has been assessed as described.[36] Total number of microparticles collected from each inlet/outlet was normalized against its corresponding cell count (Figure S4B). A slight decrease in microparticle concentration was observed in the center outlet, whereas a 5-fold increase in the microparticle count was found in the side outlet (Figure 4C, $p<0.05$). The effect of sorting on individual blood microparticle content is presented in Figure S4B.

DISCUSSIONS

In this study, we successfully quantified how RBC deformability distribution shifted over blood storage time, which can be projected into the post-transfusion *in vivo* RBC retention. For the first time, we provide clear evidence of subpopulations with dissimilar storage lesion in stored blood. Moreover, we connected single-cell level RBC deformability with other important clinical measurements including osmotic fragility and microparticle analysis, demonstrating deformability cytometry as a viable tool for monitoring blood storage lesion at individual cell level. Finally, we demonstrated a microfluidic cell separation technique to segregate the RBC subgroups with a high degree of storage lesion and other undesirable factors such as microparticles. Our results not only provided deeper understanding of the process of blood storage lesion, but also suggested a viable strategy to reduce risks related to blood transfusion, improving clinical outcomes.

The relevance of single cell deformability and spleen RBC clearance

Besides RBC hemolysis and the release of toxic heme, the "mechanical sensing" of old and abnormal RBCs in spleen is an important mechanism for the clearance of RBCs.[9] Deplaine *et. al* demonstrated that the *in vivo* clearance of old or abnormal RBCs in human spleen can be closely mimicked *in vitro* using the microbead filtration method, highlighting the important role of deformability in splenic RBC retention [9]. In the same study, the author also established a clear correlation between RBC deformability and retention rate by comparing fresh and old banked RBCs.[9] Deformability is therefore a critical and useful parameter in the understanding of post-transfusion *in vivo* RBC clearance.

In our population-based single RBC deformability analysis, RBC deformability was found to be fairly stable over the first three weeks (*i.e.* 21 days) of storage time. Significant decrease in overall deformability only became apparent starting week 4, when the mean transit velocity dropped by more than 50%, resulting in a shift in the overall deformability distribution (figure S1B, left panel). The bulk-level deformability shift (in terms of the mean value) is consistent with an independent study by Frank *et al.*[3] using ektacytometry. Yet, this bulk-level measurement showed a much more modest deformability decrease (in terms of elongation index), presumably due to the significant inhomogeneity of blood storage lesion observed from our single-cell level data.

With single-cell level deformability information, we could then estimate RBC clearance rate for a given stored blood sample, using different mathematical and statistical approaches. Figure 1B was obtained using first approach, approximating a threshold velocity. Our result suggested a RBC clearance rate of around 50% after a 4–6 week storage period (Figure 1B). The finding again was in good agreement with Deplaine *et al.* and Hod *et al.* in which RBC retention rates of 30% and 40% were reported in human and mice RBCs after prolonged storage time.[9, 11]

The advantage of our single-cell deformability profiling is that we can obtain a much more detailed picture on RBC retention caused by storage lesion, which are not obtainable in conventional population-wide "averaged" measurements. For example, in Figure 3, although the normalized velocity in side outlet was 0.73, only 27% slower than the unsorted RBCs,

we observed a significant change in the velocity distribution. In the retention rate analysis, the projected retention rate increased from 41% in the unsort sample to 66% in the side outlet (Figure 3A). On the other hand, even we observed a 12% velocity increase in center outlet as compared to the unsorted inlet, the change in projected retention was insignificant (from 41% to 39%, Figure 3A).

Finally, it should be noted that the deformability we reported using a microfluidic device with multiple constrictions may not be equivalent as compared to other deformability measurements such as ektacytometry, micropipette aspiration, or optical tweezers. Our deformability measurement is closer to the *in vivo* dynamic filtration process through probing RBCs under flow.[15] Besides membrane shear modulus, which is typically reported by micropipette aspiration and optical tweezers, RBC geometry also plays a significant role in influencing our measurement.

Different RBC deformability subgroups exhibit dissimilar blood hemolysis values

In this study we also demonstrate that, for the first time, undesirable blood components resulting from blood storage lesion (stiffened RBCs and microparticles) can be separated and enriched in a continuous filterless process. .

Banked RBCs with four to six week storage time were passed through our microfluidic blood margination (μBM) sorter such that the center and side channels collected distinctly different RBC subgroups (p<0.001, Figure 3A). We then map these two distinct deformability subgroups with osmotic fragility measurement, and confirmed that the less deformable RBCs collected in the side outlet were also more susceptible to osmotic hemolysis (Figure 4B, left panel).

The strong correlation between RBC deformability subgroups and osmotic hemolysis is likely associated with the increased subpopulation of echino-spherocytes collected in the side outlets (Figure 4A). Spherocytic RBCs often exhibit significantly lower deformability [20]. In the meantime, these spherocytic cells with reduced S/V and increased membrane fluctuation would be more fragile as compared to the normal discocytes[41]. Therefore, the elevated osmotic fragility measured from the side outlet is likely due to an increased fraction of stiffer RBCs which may have transformed into echino-spherocytes over prolonged storage time.

Cell-based deformability sorting vs. conventional blood washing

The development of a cell-based deformability sorting system, which is capable of enriching and separating different deformability subgroups, also has promising potential to be used for blood cleansing in clinical settings.

In the past, blood washing has long been performed in clinical practice to remove RBC debris and reduce plasma proteins[45]. However only recently, hemolysis and cell-free hemoglobin were identified to play a significant risk factor during blood transfusion[14], and the clinical benefit of blood washing can be largely attributed to the reduction of plasma iron content (present within microparticles).[45] Nevertheless, standard RBC washing also raises certain clinical concerns: it puts cells through high mechanical shear stress and could

increase subsequent post-transfusion hemolysis *in vivo.*[46] For example, a recent study by Cortés-Push *et al.* revealed that washing fresh blood could indeed increase plasma cell-free hemoglobin *in vivo*, worsening clinical outcomes instead. Besides, the inability to specifically remove old or abnormal RBCs is another shortcoming of conventional RBC washing: the procedure is designed to remove only plasma-borne cell-free hemoglobin, but fails to remove stiffened and fragile RBCs that are likely to release toxic heme *in vivo* post transfusion.

Our deformability-based sorting approach overcomes both limitations of standard blood washing and has the potential to make a real beneficial impact in clinical setting: firstly, the deformability-based sorting device impose minimal mechanical damage to the cells. The device was operated at 5 μl/min, mimicking *in vivo* leukocyte margination in blood capillaries.[32] Secondly, the system can remove marginated microparticles and small amount of plasma volume containing cell-free hemoglobin as well as old or stiffened RBCs that are likely to break down and release free heme *in vivo* if transfused.

With the additional prefiltration and removal of old cells, we anticipate our sorting system to achieve even better outcomes than the standard washing method. Preliminarily in this study, we demonstrated promising results after sorting more than 4-week old blood that the side outlet (i.e. waste channel) successfully enriched the most fragile cell subpopulations with highest osmotic fragility. Significantly higher microparticle concentration was also observed in the side outlet, demonstrating a significant level of removal. On the other hand, no considerable adverse sorting effect was detected on fresher (i.e. less than 4-week-old) RBCs as shown in Figure S4A.

In human applications, large volume blood (i.e. in the order of liters) cleansing is imperative. We demonstrated the ability to multiplex our cell sorting technology to achieve ultrahigh throughput. Blood margination is a passive cell separation technique, which can be readily scaled up with multiple channels of independent filtration performance. Through channel parallelization, we achieved 100 to 200-fold higher throughput (~30–60 mLh^{-1}) in a 16-channel margination platform (supplementary video). Unique design features include the radial arrangement of channels for common single blood inlet and easy collection of filtered blood from all channels from the bottom. We envision further multiplexing by stacking layers of channel or connecting multiple stacked units in a single cartridge.

We also note that the current version of the sorting device was designed to demonstrate the ability to enrich the stiff RBC subpopulations in the side outlet as a distinct contrast to unsorted RBCs. The side outlets were therefore purposely made very narrow to ensure a fairly pure population of old RBCs would be directed to the side. Consequently, we observed very promising differences in terms of RBC deformability, morphology, osmotic fragility and microparticle concentration when we compared samples collected from side outlets with unsorted inlet sample. However, given that over 80–90% of RBCs would enter the center outlet, we were not able to conclude significant improvement RBCs collected from center outlet. For enhanced clinical benefits, the focus could shift to the purification of the deformable subgroup to the center outlet. This can be done by repositioning the outlet channel split to make a narrower center outlet and correspondingly wider side outlets. In

such a way, we may only be able to utilize a smaller fraction of old stored blood, but it allows a more selective center channel for efficient blood cleansing.

Differential sorting benefits on old vs. fresh RBCs

The sorting effects were found to be different with different ages of stored RBCs. For example, a consistently lower velocity in the side outlet was only observed when processing RBCs older than 28 days (Figure S2A). Similarly, only for older blood samples (>28days), osmotic fragility test showed both improvement in the center outlet and worsening in the side outlet (Figure 4B, S4A). The differential sorting benefits on old versus fresh RBCs can be understood from the sorting device design and operation principle, as well as time-dependent differences in RBC subpopulations.

The operation principle for the deformability based sorting device is to allow more fluid-like soft RBCs to flow at the axis center, pushing the more particle-like stiff RBCs to the side walls. The mechanical differentiation between "soft" and "stiff" RBCs is therefore important to attain optimal sorting results. In freshly stored blood, most RBCs retained their biconcave morphology and were reasonably "soft" (Figure 1D), that very few cells could be classified as "stiff" enough for the margination effect to take place. For older blood stored for more than 28 days, a significant subpopulation underwent discocyte-echinocyte transformation. These echino-spherocytes have significantly stiffened cell membrane[20], and their spherical shape made them more particle-like, differentiating them further from normal biconcave RBCs. With a reasonable fraction of echino-spherocytes, the margination device could then efficiently push these significantly stiffer RBCs to the side walls and eventually concentrated them into the side outlets.

Supplementary Material

Refer to Web version on PubMed Central for supplementary material.

Acknowledgments

References

1. Solomon SB, Wang D, Sun J, Kanias T, Feng J, Helms CC, Solomon MA, Alimchandani M, Quezado M, Gladwin MT, Kim-Shapiro DB, Klein HG, Natanson C. Blood. 121:1663–1672. [PubMed: 23255558]

2. Department of Health and Human Services; Washington, DC: 2013.

3. Frank SM, Abazyan B, Ono M, Hogue CW, Cohen DB, Berkowitz DE, Ness PM, BVM. Anesthesia & Analgesia. 2013

4. Dumont LJ, AuBuchon JP. Transfusion. 2008; 48:1053–1060. [PubMed: 18298603]

5. Farges E, Grebe R, Baumann M. Clinical Hemorheology and Microcirculation. 2002; 27:1–11. [PubMed: 12237485]

6. Kim-Shapiro DB, Lee J, Gladwin MT. Transfusion. 2011; 51:844–851. [PubMed: 21496045]

7. Offner P. Crit Care. 2004; 8:1–3. [PubMed: 14975035]

8. Luten M, Roerdinkholder-Stoelwinder B, Schaap N, de Grip W, Bos H, Bosman G. Transfusion. 2008; 48:1478–1485. [PubMed: 18482180]

9. Deplaine G, Safeukui I, Jeddi F, Lacoste F, Brousse V, Perrot S, Biligui S, Guillotte M, Guitton C, Dokmak S, Aussilhou B, Sauvanet A, Cazals Hatem D, Paye F, Thellier M, Mazier D, Milon G, Mohandas N, Mercereau-Puijalon O, David PH, Buffet PA. Blood. 2011; 117:e88–e95. [PubMed: 21163923]

10. Huang S, Undisz A, Diez-Silva M, Bow H, Dao M, Han J. Integrative Biology. 2013; 5:414–422. [PubMed: 23254624]

11. Hod EA, Zhang N, Sokol SA, Wojczyk BS, Francis RO, Ansaldi D, Francis KP, Della-Latta P, Whittier S, Sheth S, Hendrickson JE, Zimring JC, Brittenham GM, Spitalnik SL. Blood. 2010; 115:4284–4292. [PubMed: 20299509]

12. Salzer U, Zhu R, Luten M, Isobe H, Pastushenko V, Perkmann T, Hinterdorfer P, Bosman GJCGM. Transfusion. 2008; 48:451–462. [PubMed: 18067507]

13. Latham JT, Bove JR, Weirich FL. Transfusion. 1982; 22:158–159. [PubMed: 7071919]

14. Kanias T, Gladwin MT. Transfusion. 2012; 52:1388–1392. [PubMed: 22780890]

15. Huang S, Amaladoss A, Liu M, Chen H, Zhang R, Preiser P, Dao M, Han J. Infection and Immunity. 2014

16. Donadee C, Raat NJH, Kanias T, Tejero J, Lee JS, Kelley EE, Zhao X, Liu C, Reynolds H, Azarov I, Frizzell S, Meyer EM, Donnenberg AD, Qu L, Triulzi D, Kim-Shapiro DB, Gladwin MT. Circulation. 2011; 124:465–476. [PubMed: 21747051]

17. Baron DM, Beloiartsev A, Nakagawa A, Martyn T, Stowell CP, Malhotra R, Mayeur C, Bloch KD, Zapol WM. Critical Care Medicine. 2013; 41:2492. [PubMed: 23887236]

18. Rother RP, Bell L, Hillmen P, Gladwin MT. JAMA. 2005; 293:1653–1662. [PubMed: 15811985]

19. Herring JM, Smith SA, McMichael MA, O'Brien M, Ngwenyama TR, Corsi R, Galligan A, Beloshapka AN, Deng P, Swanson KS. Veterinary Clinical Pathology. 2013; 42:163–169. [PubMed: 23560818]

20. Park Y, Best CA, Auth T, Gov NS, Safran SA, Popescu G, Suresh S, Feld MS. Proceedings of the National Academy of Sciences. 2010; 107:1289–1294.

21. Izzo P, Manicone A, Spagnuolo A, Lauta VM, Pasquale AD, Monte DD. Clinical Hemorheology and Microcirculation. 1999; 21:335–339. [PubMed: 10711766]

22. Bessis MN, Feo MC. Blood Cells. 1980; 6:315–327. [PubMed: 7397390]

23. Berezina TL, Zaets SB, Morgan C, Spillert CR, Kamiyama M, Spolarics Z, Deitch EA, Machiedo GW. Journal of Surgical Research. 2002; 102:6–12. [PubMed: 11792145]

24. Hochmuth RM. Journal of Biomechanics. 2000; 33:15–22. [PubMed: 10609514]

25. Park Y, Diez-Silva M, Popescu G, Lykotrafitis G, Choi W, Feld MS, Suresh S. Proceedings of the National Academy of Sciences. 2008; 105:13730–13735.

26. Mills JP, Diez-Silva M, Quinn DJ, Dao M, Lang MJ, Tan KSW, Lim CT, Milon G, David PH, Mercereau-Puijalon O, Bonnefoy S, Suresh S. Proceedings of the National Academy of Sciences. 2007; 104:9213–9217.

27. Bow H, Pivkin IV, Diez-Silva M, Goldfless SJ, Dao M, Niles JC, Suresh S, Han J. Lab on a Chip. 2011; 11:1065–1073. [PubMed: 21293801]

28. Kwan JM, Guo Q, Kyluik-Price DL, Ma H, Scott MD. American Journal of Hematology. 2013; 88:682–689. [PubMed: 23674388]

29. Guo Q, Duffy SP, Matthews K, Santoso AT, Scott MD, Ma H. Journal of Biomechanics. 47:1767–1776. [PubMed: 24767871]

30. Bow H, Pivkin IV, Diez-Silva M, Goldfless SJ, Dao M, Niles JC, Suresh S, Han J. Lab on a Chip. 2011; 11:1065–1073. [PubMed: 21293801]

31. Hou HW, Gan HY, Bhagat AAS, Li LD, Lim CT, Han J. Biomicrofluidics. 2012; 6

32. Hou HW, Bhagat AAS, Lin Chong AG, Mao P, Wei Tan KS, Han J, Lim CT. Lab on a Chip. 2010; 10:2605–2613. [PubMed: 20689864]

33. Vettore L, Zanella A, Molaro GL, De Matteis MC, Pavesi M, Mariani M. Acta Haematol. 1984; 72:258–263. [PubMed: 6438993]

34. Zerhouni F. European journal of haematology. 1988; 41:510–511. [PubMed: 3208875]

35. Zwart A, van Assendelft OW, Bull BS, England JM, Lewis SM, Zijlstra WG. J Clin Pathol. 1996; 49:271–274. [PubMed: 8655699]

36. Xiong Z, Oriss TB, Cavaretta JP, Rosengart MR, Lee JS. Vox sanguinis. 2012; 103:42–48. [PubMed: 22236393]

37. Xiong Z, Cavaretta J, Qu L, Stolz DB, Triulzi D, Lee JS. Transfusion. 2011; 51:610–621. [PubMed: 20738825]

38. Beutler E, Kuhl W, West C. Blood. 1982; 59:1141–1147. [PubMed: 7082820]

39. Li L, Su J, Li J, Peng F, Wu H, Ye D, Chen H. RSC Advances. 2012; 2:7161–7165.

40. Bieri VG, Wallach DFH, Lin PS. Proceedings of the National Academy of Sciences. 1974; 71:4797–4801.

41. Safeukui I, Buffet PA, Deplaine G, Perrot S, Brousse V, Ndour A, Nguyen M, Mercereau-Puijalon O, David PH, Milon G, Mohandas N. Blood. 2012; 120:424–430. [PubMed: 22510876]

42. Park Y, Best CA, Badizadegan K, Dasari RR, Feld MS, Kuriabova T, Henle ML, Levine AJ, Popescu G. Proceedings of the National Academy of Sciences. 2010; 107:6731–6736.

43. Buffet PA, Safeukui I, Deplaine G, Brousse V, Prendki V, Thellier M, Turner GD, Mercereau-Puijalon O. Blood. 2011; 117:381–392. [PubMed: 20852127]

44. Wikibooks. Data Mining Algorithms in R. http://en.wikibooks.org/wiki/Data_Mining_Algorithms_In_R/Clustering/K-Means

45. Cortés-Puch I, Wang D, Sun J, Solomon SB, Remy KE, Fernandez M, Feng J, Kanias T, Bellavia L, Sinchar D, Perlegas A, Solomon MA, Kelley WE, Popovsky MA, Gladwin MT, Kim-Shapiro DB, Klein HG, Natanson C. Blood. 2014; 123:1403–1411. [PubMed: 24366359]

46. Harm SK, Raval JS, Cramer J, Waters JH, Yazer MH. Transfusion Medicine. 2012; 22:181–185. [PubMed: 22188550]
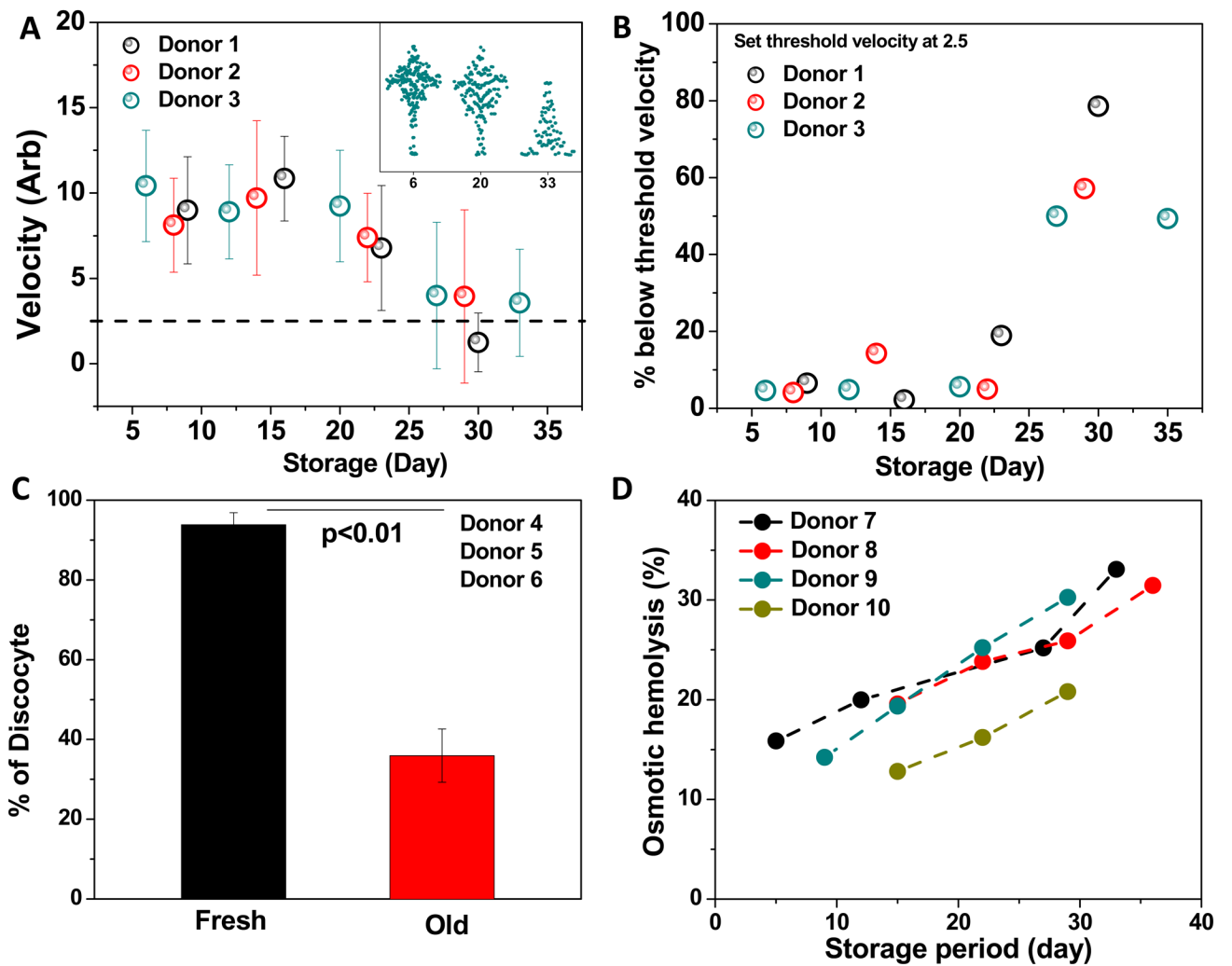
47. R Development Core Team 2011

Figure 1. Changes in deformability, morphology, and osmotic fragility over time
Figure 1. Storage time dependent changes in RBC deformability (A, donor 1–3), morphology (C, donor 4–6), and osmotic fragility (D, donor 7–9) were traced for up to 35 days. RBC clearance post transfusion was projected based on *in vitro* deformability measurement (B, donor 1–3)
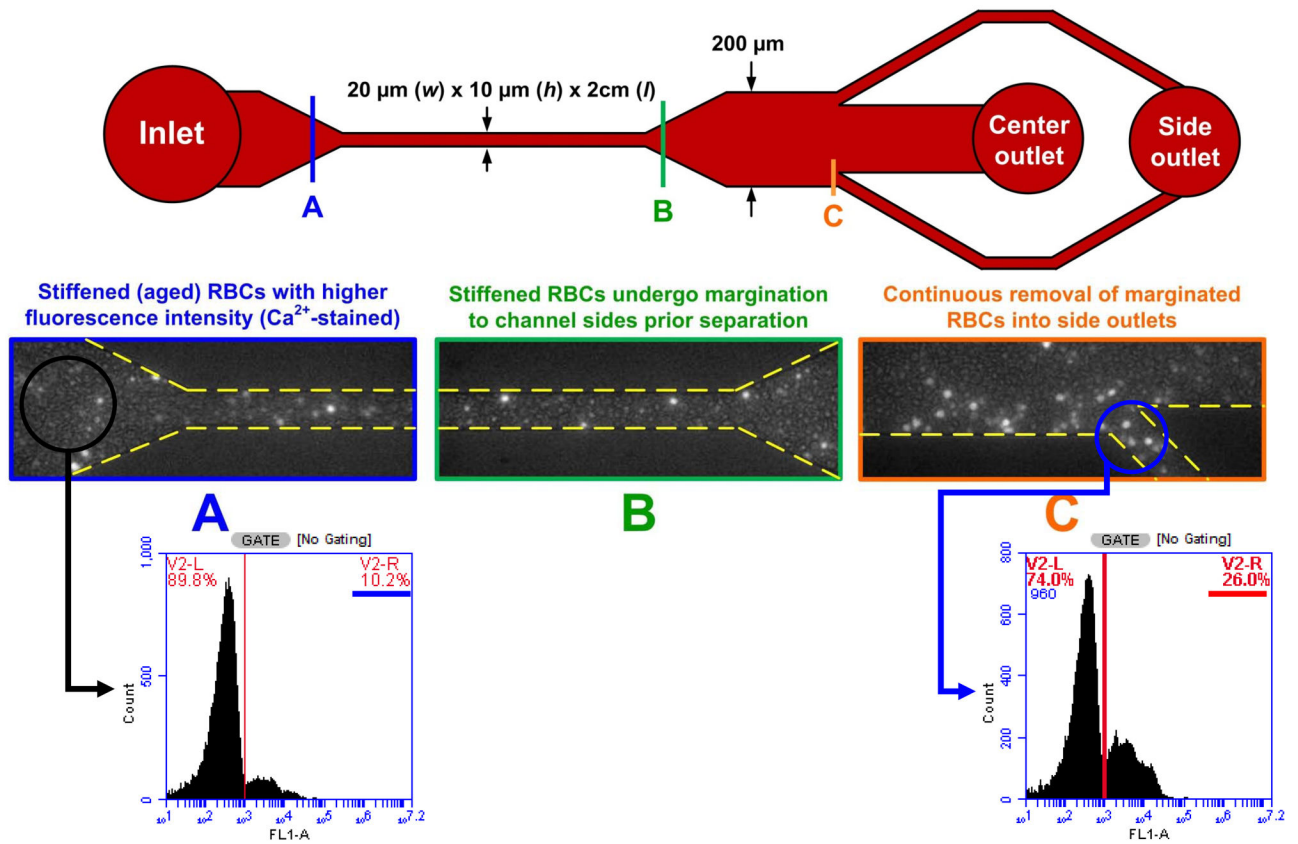
Figure 2. Deformability Sorter

Figure 2. Deformability sorter schematics. 90% fresh blood (unstained) and 10% old blood (stained bright) were premixed before loading into the device. Section A, B, C illustrates the inlet channel, straight margination zone, and the outlet channel (side channel), respectively. 3 fold enrichment of old blood was observed in the side outlet according to FACS analysis.
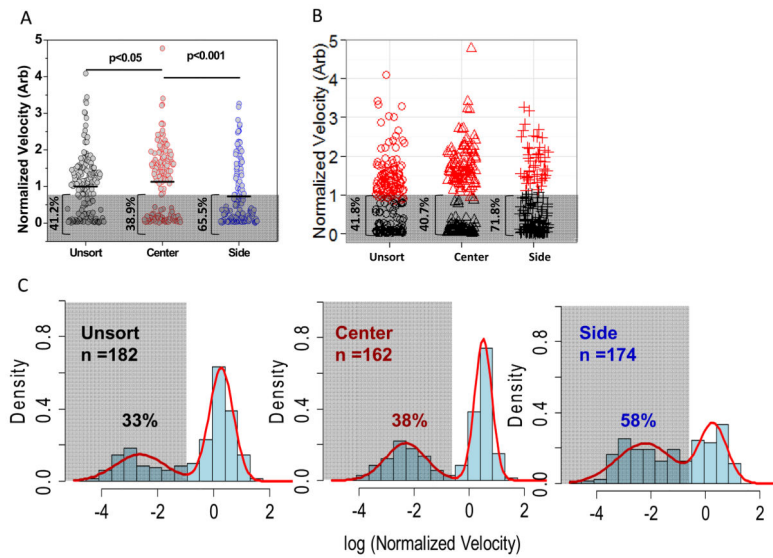
Figure 3. Deformability Sorting and Subgroup Clustering
Figure 3. RBC deformability profile after margination device sorting (A). By setting a
hypothetical velocity threshold at normalized velocity of 0.8, the percentages of "slow"
RBCs moving below threshold velocity were 41.2%, 38.9% and 65.5% respectively in
unsort, center and side channels. Standard K-means clustering was performed and identified
similar percentages of "slow" RBCs in respective channels (B, 41.8%, 40.7%, and 71.8%).
Finally biostatistical analysis was performed that velocity data were fitted into bimodal
distribution after log transform. The "slow" RBCs were denoted by the lower hump and
corresponding percentages in each channel were labeled. (C). Both clustering and bimodal
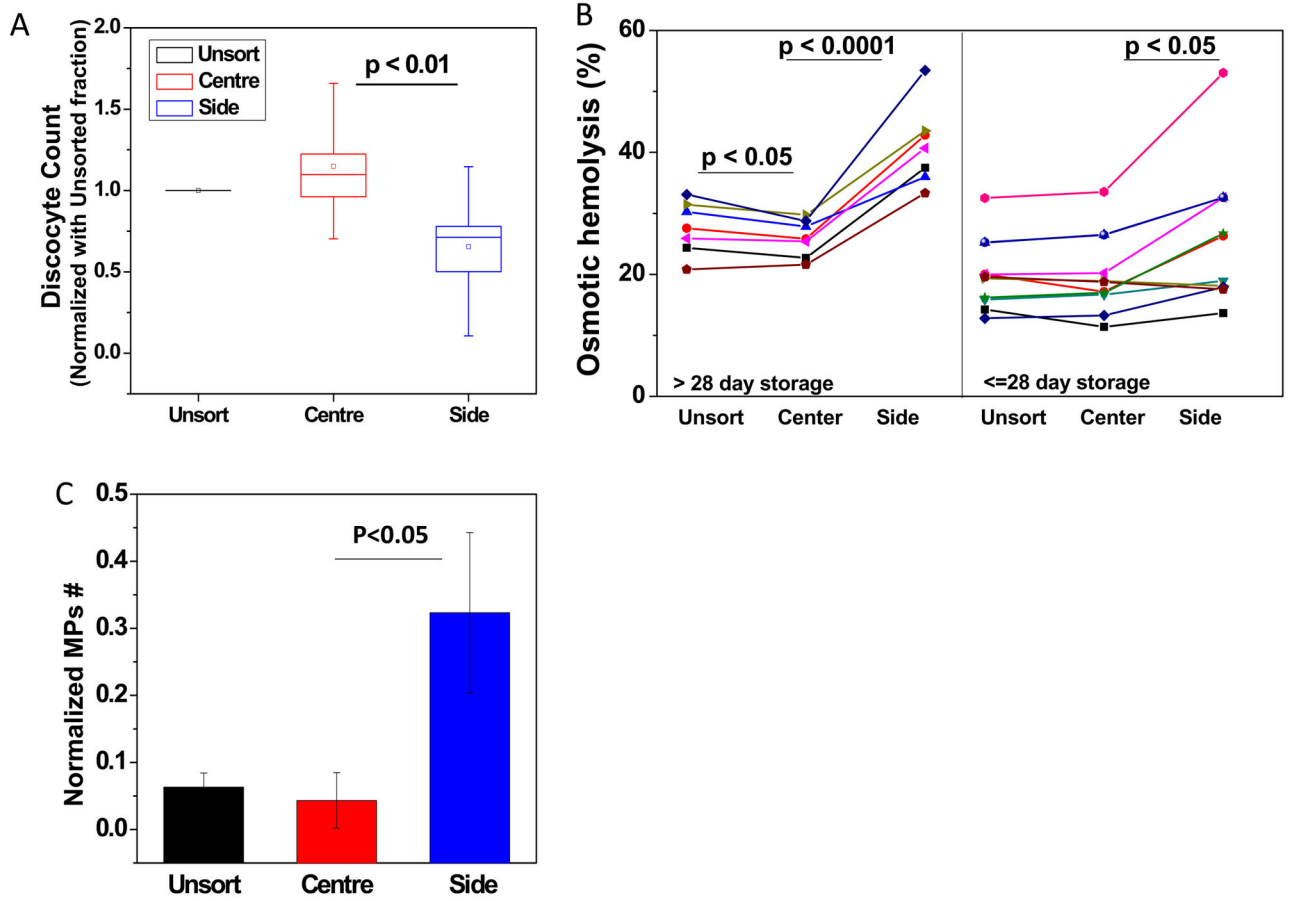fitting were performed using R version 2.13. [47]

Figure 4. RBC morphology, fragility and microparticle concentration after sorting
Figure 4. Effect of deformability sorting on old stored RBC morphology (A), osmotic fragility (B), and microparticle content (C). RBCs collected by the side channel show with poor morphology (lower discocytes count), high fragility as well as high microparticle content.

Author Manuscript

Author Manuscript

Author Manuscript

Author Manuscript

Table 1

RBC subpopulation clustering using statistical analysis.

$$f(x) = a_1 \frac{1}{\sqrt{2\pi}c_1} e^{-\frac{(x-b_1)^2}{2c_1^2}} + a_2 \frac{1}{\sqrt{2\pi}c_2} e^{-\frac{(x-b_2)^2}{2c_2^2}}$$

	Unsort	Center	Side
% of "slow" RBCs (a1)	33%	38%	58%
Lower ave. velocity in log (b1)	−2.62	−2.31	−2.23
Higher ave. velocity in log (b2)	0.27	0.51	0.29